

The Solar Photospheric-to-Coronal Fe abundance from X-ray Fluorescence Lines

K. J. H. Phillips¹

¹*Mullard Space Science Laboratory, University College London, Holmbury St Mary, Dorking RH6 5NT, UK*

Submitted 2011 November

ABSTRACT

The ratio of the Fe abundance in the photosphere to that in coronal flare plasmas is determined by X-ray lines within the complex at 6.7 keV (1.9 Å) emitted during flares. The line complex includes the He-like Fe (Fe XXV) resonance line w (6.70 keV) and Fe K α lines (6.39, 6.40 keV), the latter being primarily formed by the fluorescence of photospheric material by X-rays from the hot flare plasma. The ratio of the Fe K α lines to the Fe XXV w depends on the ratio of the photospheric-to-flare Fe abundance, heliocentric angle θ of the flare, and the temperature T_e of the flaring plasma. Using high-resolution spectra from X-ray spectrometers on the *P78-1* and *Solar Maximum Mission* spacecraft, the Fe abundance in flares is estimated to be 1.6 ± 0.5 and 2.0 ± 0.3 times the photospheric Fe abundance, the *P78-1* value being preferred as it is more directly determined. This enhancement is consistent with results from X-ray spectra from the *RHESSI* spacecraft, but is significantly less than a factor 4 as in previous work.

Key words: Sun: abundances — Sun: corona — Sun: flares — Sun: X-rays, gamma rays — line: identification.

1 INTRODUCTION

The solar iron abundance remains a subject for discussion in the literature, both the value obtained from photospheric spectra and that from coronal spectra, generally in the X-ray or extreme ultraviolet spectral regions. Recent photospheric abundance determinations (Asplund et al. 2009) using three-dimensional photospheric models give $A(\text{Fe}) = 7.50 \pm 0.04$ (Asplund et al. 2009) and 7.52 ± 0.06 (Caffau et al. 2011) (abundances are here expressed logarithmically, on a scale where $A(\text{H}) = 12$), less by up to 60% (0.2 dex) than values current as recently as the mid-1990s (Blackwell et al. 1995). Since the 1980s, it has become widely recognized that solar coronal element abundances differ from photospheric by factors that depend on the first ionization potential (FIP) of the element, with the coronal abundances of low-FIP (i.e. $\lesssim 10$ eV) being enhanced but with the coronal abundances of high-FIP elements that are similar to their photospheric abundances. The reviews by Feldman (1992) and Feldman & Laming (2000) give enhancement factors for some low-FIP elements of up to 4. However, low-altitude coronal flare plasmas and other energetic events are stated to have photospheric abundances, while Feldman et al. (1990) find that the corona directly above a sunspot also has photospheric abundances but neighbouring coronal regions have low-FIP elements with enhanced abundances. Iron, with a FIP of 7.9 eV, is expected to have a low-FIP element behaviour. A recent analysis (Phillips & Dennis 2011) of solar flare spectra observed by the *Reuven Ramaty High Energy Solar Spectroscopic Imager* (*RHESSI*) gives a rather different picture. *RHESSI* spectra cover an energy range ~ 3 keV to 17 MeV, and have a spectral resolution of $\Delta E \sim 1$ keV; in the soft X-ray range ($\sim 3 - 10$ keV, $1.2 - 4$ Å), a strong complex of Fe lines, forming an emission line feature at 6.7 keV (1.85 Å), is evident on a continuum made up of free-free and free-bound emission. Under certain circumstances – late in the flare development, with the *RHESSI* thin attenuators in place – an isothermal assumption for the flare’s emitting plasma appears to be valid, and with electron temperature T_e and emission measure ($EM = N_e^2 V$, where N_e = electron density, V = the emitting volume) estimated from the continuum, the Fe abundance can be determined. Analysis of nearly 2000 spectra observed during 20 flares led to the value $A(\text{Fe}) = 7.91 \pm 0.10$, with very little variation from flare to flare. This abundance is a factor of 2.6 ± 0.6 more than recent photospheric abundance estimates, significantly less than 4.

Phillips et al. (1994) describe a means of obtaining the photospheric-to-flare Fe abundance ratio directly using the Fe xxv resonance line w (transition $1s^2\ ^1S_0 - 1s2p\ ^1P_1$), which is frequently the strongest line making up the 6.7 keV line complex, and a feature at 7.06 keV (1.76 Å) made up of Fe K β lines, with inner-shell transition ($1s - 3p$) and formed by fluorescence of the photosphere by the coronal hot flare plasma. Spectra from the Bragg Crystal Spectrometer on the Japanese *Yohkoh* spacecraft were used to find that the flare Fe abundance was no more than a factor 2 higher than the photospheric abundance. A preliminary analysis (Phillips et al. 1995) of Fe xxv and Fe K α line spectra observed by the SOLFLEX instrument on *P78-1* spacecraft and the Bent Crystal Spectrometer (BCS) on *Solar Maximum Mission* (*SMM*) points to the photospheric and coronal Fe abundances being equal.

Here the analysis of Phillips et al. (1995) is revisited, with the theory and observations of the ratio of the Fe K α lines to the Fe xxv w re-examined. The original observations from the SOLFLEX instrument on the *P78-1* spacecraft are used, together with newly analyzed observations from the *Solar Maximum Mission* Bent Crystal Spectrometer. The photospheric-to-flare abundance ratios are now consistent with the flare Fe abundance estimates from *RHESSI*.

2 THEORY OF LINE FORMATION

The inner-shell K α and K β lines visible in solar flare X-ray spectra are formed when K ($nl = 1s$) shell electrons in the neutral or once-ionized Fe atoms in the photosphere are removed. The K-shell electron may be ejected by either electrons or X-ray photons having energies > 7.11 keV. The vacancy in the K-shell is filled by an electron in the L ($nl = 2p$) or M ($nl = 3p$) shell; this results in either the emission of a photon or a re-arrangement of the remaining electrons with the emission of an Auger electron. In the case of the L–K transition, the photon emission forms two lines, with K α_1 at energy 6.404 keV (1.936 Å, transition $1s_{1/2} - 2p_{3/2}$) and K α_2 at energy 6.391 keV (1.940 Å, $1s_{1/2} - 2p_{1/2}$). Their intensity ratio is K α_1 :K $\alpha_2 = 2 : 1$. The M–K transition results in K β line emission, with the most intense components being the K β_1 and K β_3 lines at 7.057 keV (1.76 Å). The relative probability of photon emission is expressed by the fluorescence yield ω_K which for Fe is 0.31 (Fink et al. 1966). This rapidly increases with atomic number (roughly as Z^4), so explaining the fact that the fluorescence lines of Fe are the only ones ever to be observed with solar X-ray crystal spectrometers (Ni, with higher Z and larger ω_K , has an abundance about 20 times less than Fe).

For solar flares, the Fe inner-shell lines can be excited by energetic electrons (Phillips & Neupert 1973), such as those in the tail of the Maxwell-Boltzmann distribution in hot flare plasmas or nonthermal electrons present at the flare impulsive stage, or by photons from the flare plasma incident on the photosphere (Bai 1979). In the case of the latter, a strong dependence on the flare heliocentric angle would be expected, with limb flares having zero or very small fluorescence emission. This centre-to-limb dependence has been observed from spectral data from the *SMM* and *Yohkoh* crystal spectrometers (Parmar et al. 1984; Phillips et al. 1994), and so it may be presumed that fluorescence emission predominates. Indeed, only one ambiguous case has been cited of a flare during its impulsive stage for which nonthermal electron excitation of the Fe K α lines has been observed (Emslie et al. 1986).

The Fe K α or K β fluorescence emission is formed in a layer of the solar atmosphere where X-rays with energies > 7.11 keV are absorbed by Fe atoms or ions. The absorption cross sections above and below the 7.11 keV edge by Fe indicate that absorption effectively occurs at a mass column density of ~ 1 g cm $^{-2}$, which in the VAL (Vernazza et al. 1981) “average” model solar atmosphere and for the photospheric Fe abundance (Asplund et al. 2009; Caffau et al. 2011) is located at about 200 km above the $\tau_{5000} = 1$ level, on the photospheric side of the temperature minimum.

The theory for the formation of the Fe K lines by fluorescence has been described by Bai (1979), whose theory was based on a Monte Carlo analysis. We briefly outline it here. The flux of the K α lines at the distance of the Earth D is

$$F(\text{K}\alpha) = \frac{B\Gamma f(\theta, h)}{1 + \alpha f(\theta, h)} \frac{1}{4\pi D^2} \int_{7.11}^{\infty} I_{>7.11} EM(E) dE \quad \text{photons cm}^{-2} \text{ s}^{-1} \quad (1)$$

where the branching ratio B for K α line emission is 0.882 (0.118 for K β line emission: Bambynek et al. (1972)), Γ is the efficiency of the production of K α line emission (equal to the ratio of line emission to the total emission at energies greater than the K-shell ionization energy, 7.11 keV), and $f(\theta, h)$ is a function describing the dependence of the line emission on the heliocentric angle θ and height h above the photosphere of the hot flare plasma fluorescing the photosphere. The factor $[1 + \alpha f(\theta, h)]$ corrects for Compton-scattered albedo photons contributing to the total emission with energy > 7.11 keV, $I_{>7.11}$ times the flare’s volume emission measure EM . This emission is taken to be thermal in Bai (1979)’s analysis, and is made up of free–free and free–bound continua, with negligible line emission. In this analysis, $I_{>7.11}$ was taken to be the continuum emission given by the CHIANTI database and software package (Dere et al. 1997, 2009) rather than the analytical expression derived by Phillips et al. (1994). The emission measure EM is $N_e^2 V$ where N_e is the electron density and V the flare’s emitting volume. The fluorescence efficiency Γ is a function of the flare plasma height h , the photospheric Fe abundance $N(\text{Fe})/N(\text{H})$, and the temperature T_e of the hot plasma, assumed isothermal. The photospheric Fe abundance affects the value of Γ in a nearly linear way; $A(\text{Fe}) = 7.60$ (or $N(\text{Fe})/N(\text{H}) = 4.0 \times 10^{-5}$) was used in Bai (1979)’s analysis. We adapted

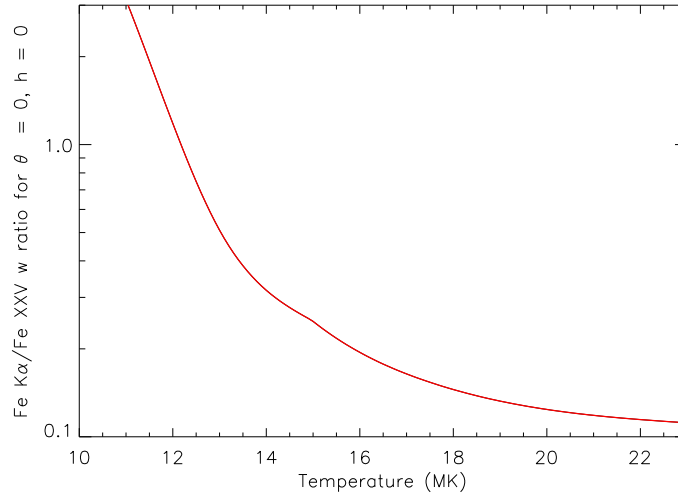


Figure 1. Dependence of the ratio R of Fe $K\alpha$ line flux to Fe XXV w line flux for disk-centre ($\theta = 0$) and zero height flares.

this using $\Gamma' = \Gamma \times [N(\text{Fe})/N(\text{H})]_{\text{phot}}/[N(\text{Fe})/N(\text{H})]_{\text{Bai}}$ where $[N(\text{Fe})/N(\text{H})]_{\text{Bai}} = 4.0 \times 10^{-5}$ (corresponding to $A(\text{Fe}) = 7.60$) and $[N(\text{Fe})/N(\text{H})]_{\text{phot}}$ was set equal to 3.2×10^{-5} , corresponding to Asplund et al. (2009)'s value ($A(\text{Fe}) = 7.50$).

The Fe XXV w line is emitted by the flare plasma by collisional excitation processes. The w line flux is then given by

$$F(w) = \frac{G(T_e) \times EM'}{4\pi D^2} \quad (2)$$

with $G(T_e)$ the contribution function for the w line including high- n dielectronic satellite lines that are spectroscopically indistinguishable from line w . The emission measure EM' is taken to be equal to EM for the emission at energies > 7.11 keV, i.e. the emitting plasma is assumed to be isothermal. The justification for this is from *RHESSI* flare spectra which show this to be a good approximation for flares in their decay stage (Phillips & Dennis 2011). For the Fe XXV w line alone, $G(T_e)$ is given by

$$G(T_e) = \frac{N(\text{Fe}_e^{+24})}{N(\text{Fe}^{+24})} \frac{N(\text{Fe}^{+24})}{N(\text{Fe})} \left[\frac{N(\text{Fe})}{N(\text{H})} \right]_{fl} \frac{N(\text{H})}{N_e} \frac{A_{i0}}{N_e} \text{ cm}^3 \text{ s}^{-1} \quad (3)$$

where $N(\text{Fe}_e^{+24})$ is the population of the excited level of the He-like Fe ion, $N(\text{Fe}^{+24})/N(\text{Fe})$ is the He-like ion fraction. $[N(\text{Fe})/N(\text{H})]_{fl}$ is the coronal flare Fe abundance relative to H, and A_{e0} the transition probability from level e to the ground state; $N(\text{H})/N_e$ is taken to be 0.83. $G(T_e)$ was evaluated from CHIANTI, with ion fractions from Bryans et al. (2009), and the flare Fe abundance $[N(\text{Fe})/N(\text{H})]_{fl}$ (see below). Although CHIANTI has data for unresolved satellites converging on to the Fe XXV w line, these include satellites of the type $1s^2nl - 1s2pnl$ with nl with principal quantum number n up to 5. We instead used data from Bely-Dubau et al. (1982) which includes satellites with much higher n values; this is a decreasing function of T_e , e.g. equal to 50% of the Fe XXV w line $G(T_e)$ for $T_e = 17$ MK. We denote the sum of the $G(T_e)$ function for the Fe XXV w line and unresolved Fe XXIV satellites by $G'(T_e)$.

The ratio of fluxes in the Fe $K\alpha$ lines to the Fe XXV w line plus unresolved Fe XXIV satellites is then

$$\frac{F(K\alpha)}{F(w)} = R = \frac{B \Gamma' f(\theta, h)}{1 + \alpha f(\theta, h)} \frac{\int_{7.11}^{\infty} EM I_{>7.11}(E) dE}{G'(T_e)} \quad (4)$$

The ratio R is a function of T_e , the flare heliocentric angle θ and its height above the photosphere h . It is also proportional to the ratio of the photospheric Fe abundance $[N(\text{Fe})/N(\text{H})]_{\text{phot}}$ (through Γ') to the flare plasma Fe abundance, $N(\text{Fe})/N(\text{H})_{fl}$ through the $G(T_e)$ function (Eq. 3), neglecting the contribution of unresolved satellites.

The ratio R is plotted logarithmically as a function of T_e for disk-centre ($\theta = 0$) and $h = 0$ flares with photospheric and flare Fe abundances set equal (Figure 1). There is a steep decline for temperatures that are relatively low but for those considered here, $T_e = 17$ MK, attained shortly after flare peak values, the dependence is more gradual.

The dependence of R on the flare Fe abundance and θ is shown in Figure 2 for heights h of 0 and 7000 km. The flare abundances $[N(\text{Fe})/N(\text{H})]_{fl}$ chosen are the coronal value of Feldman & Laming (2000), the photospheric value of Asplund et al. (2009), and the value from *RHESSI* observations (Phillips & Dennis 2011).

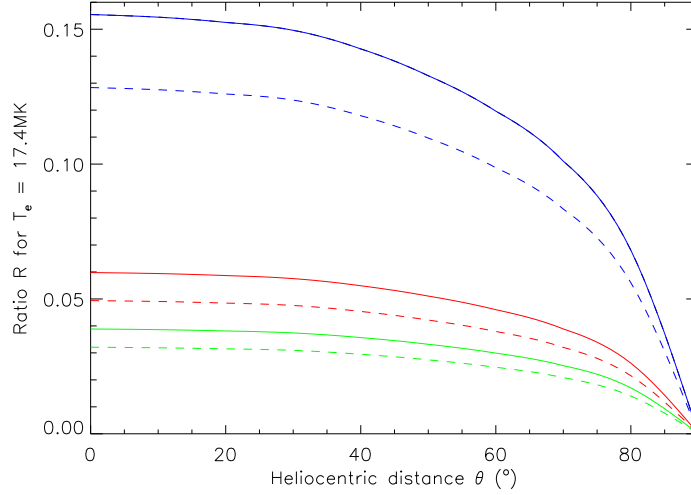


Figure 2. Dependence of the ratio R for $T_e = 17.4$ MK on heliocentric angle θ and flare abundances, equal to the abundances of Feldman & Laming (2000) (blue), Phillips & Dennis (2011) (red), and Asplund et al. (2009) (green). The dependence on flare heights is shown by the $h = 0$ (solid curves) and $h = 7000$ km (dashed curves).

3 OBSERVATIONS

Spectra over the 6.4–6.7 keV (1.85 – 1.94 Å) range, including the Fe xxv w and Fe K α lines, have been made by a number of spacecraft crystal spectrometers operating between 1979 and 1989. The flat crystal spectrometer SOLFLEX on *P78-1* scanned the range repeatedly back and forth and obtained several spectra during flares (Doschek et al. 1979). Measurements of line fluxes during a small sample of flares were made for the analysis of Phillips et al. (1995). Unfortunately, an on-line archive of the data is not available, so for the analysis here these measurements are used again. These observations allow direct comparison of the Fe xxv w and Fe K α lines which are clearly resolved.

The Bent Crystal Spectrometer (BCS) on *SMM* consisted of 8 channels, 7 covering the Fe lines of interest. A bent germanium crystal (Ge 422 crystal plane) with particular bend radius for each of these channels allowed portions of the full range to be observed, the spectra being observed by position-sensitive proportional counters. The spectral ranges are given in Table 1, together with effective areas and instrumental line broadening parameters, all based on pre-launch measurements (Acton et al. 1980). The main advantages of bent crystal spectrometers include the fact that, over a relatively short time (DGI or data gathering interval, typically a few seconds), photon counts making up a spectrum can be accumulated in each channel’s range, whereas with a scanning flat crystal spectrometer particular spectral lines are scanned at slightly different times. This advantage is most apparent during a flare’s rapid rise. Channels 4 and 7 of the BCS observed the Fe xxv w line, with channel 4 having a larger range but smaller sensitivity than channel 7. The Fe K α lines were observed in channels 2 and 3, with channel 3 having a larger wavelength range but smaller sensitivity than channel 2. Thus, to evaluate the flux ratio of the Fe K α and Fe xxv lines involves the ratio of measured effective areas of two separate channels. For this analysis, individual line fluxes were measured by best-fit Voigt functions to the line profiles using routines written in Interactive Data Language (IDL), with the Gaussian part of the function equal to the thermal Doppler broadening plus electronic broadening and the Lorentzian part approximating the crystal rocking curve (this assumption is not critical as the rocking curve width is approximately 10 times less than the thermal Doppler broadening width). Figure 3 shows spectra in channels 3 and 4 during two large flares seen by *SMM*, one near disk centre ($\theta = 16^\circ$) and the other near the west limb ($\theta = 90^\circ$). The Fe K α lines are visible only in the disk flare spectrum. These spectra are composites of channels 3 and 4. The Fe K α lines are much more conspicuous in the more sensitive channel 2 (see left panels of the figure). Fluorescence of the germanium material of the crystals by solar X-rays during flares is observed by the position-sensitive detectors as a background over all wavelengths, present in the spectra of Figure 3 as well as the SOLFLEX spectra.

For both the *P78-1* and *SMM* observations, large flares were selected with a variety of heliocentric distances. As both SOLFLEX and BCS were only coarsely collimated spectrometers, they do not give accurate solar coordinates for each flare; these were instead obtained from the coordinates of H α flares listed in the *Solar-Geophysical Data Bulletin*. Generally the correlation of the X-ray and H α flares was unambiguous but at intervals of high solar activity there were occasionally more than one H α flare occurring simultaneously; these flares were rejected from the data base. Table 2 lists the flares observed by SOLFLEX and BCS included in the analysis. Most are in 1980, near the peak of Cycle 22. Although *SMM* continued operating after 1984, when the spacecraft attitude control unit was replaced by Space Shuttle astronauts, activity had declined and BCS channel 2 had failed, so that there were few flares available for analysis.

Table 1. *SMM* Bent Crystal Spectrometer Channels

Chan. No.	Lines included	Energy range (wavelength range) keV (Å)	Effective area (cm ²)	Instrumental broadening (FWHM) in keV [Å] ¹
2	Fe K α	6.375–6.431 (1.928–1.945)	0.019	4.89 (-4) [1.48(-4)]
3	Fe XXV <i>w</i> to Fe XXI sats.	6.368–6.550 (1.893–1.947)	.0063	1.47 (-3) [4.36(-4)]
4	Fe XXI sats. to Fe K α	6.546–6.739 (1.840–1.894)	.0059	1.55 (-3) [4.35(-4)]
7	Fe XXV <i>w</i>	6.684–6.731 (1.842–1.855)	.025	6.64 (-4) [1.83(-4)]

¹ Quadratic sum of crystal rocking curve and electronic broadening.

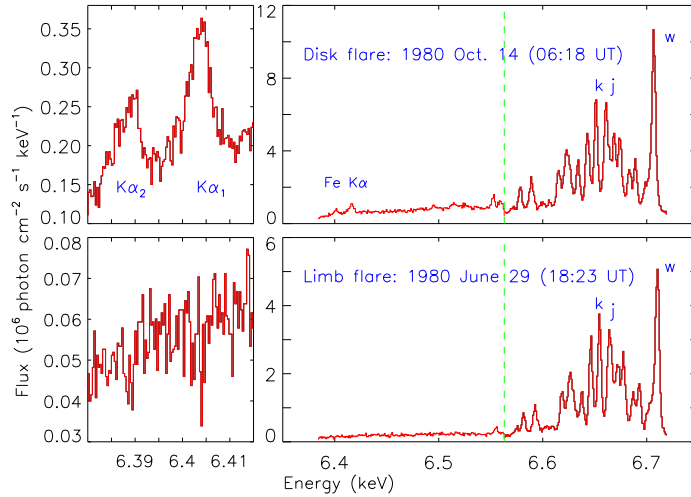


Figure 3. *SMM* BCS channels 3 and 4 spectra (right panels) for a disk flare (1980 October 14, $\theta = 16^\circ$), showing the K α lines at 6.4 keV in channel 2 (left panel), and a limb flare (1980 June 29), with no visible K α line emission. The vertical dashed green lines indicate the boundaries of channels 3 and 4. The Fe XXV *w* line (6.699 keV) and two of the Fe XXIV dielectronic satellites *j* and *k* are indicated. The region of the Fe K α lines as viewed by channel 2 are shown in the left panels. The spectra are plotted on an energy scale (abscissa) and absolute flux scale (ordinate) using the effective areas of Table 1.

4 RESULTS

Measured flux ratios R_{obs} of the Fe K α to the Fe XXV *w* line for times when the estimated temperature from the flux ratio of the Fe XXIV *j* satellite to the Fe XXV *w* line was 17 MK (corresponding to a *j/w* ratio of 0.58) are given in Table 2. A typical DGI for the observations was 16 s. For the *SMM* BCS measurements, fluxes in channels 2 and 7 only are given. The uncertainties given in the table are statistical only, estimated from the Voigt line fitting routine; they do not include other possible uncertainties in the fitting process, e.g. in placing the fluorescence background. The uncertainties in the derived ratios result from propagating those in the measured Fe K α_1 , Fe K α_2 , and Fe XXV *w* line fluxes. Corresponding measurements from channel 3 have much larger uncertainties as a result of the smaller photon count rates in this channel, as can be seen from Figure 3, and are not given in the Table. For the *P78-1* SOLFLEX observations, a notional uncertainty of 20% is assigned, based on the estimation of statistical noise of the spectra from our earlier analysis (Phillips et al. 1995).

The ratios are plotted against the flare heliocentric distance in Figure 4 with zero-height theory curves for the three Fe abundances chosen from Figure 2. The justification for choosing zero height is from *Skylab* images with the S082A slitless extreme ultraviolet spectrograph (e.g. Widing & Cheng (1974)) which imaged a number of flares in the 192 Å Fe XXIV line, showing very small heights at the temperature of this line which is almost as hot as the Fe XXV *w* line. A number of limb flares were observed with no evidence for the Fe K α lines; they are shown as the single point with zero ratio at $\theta = 90^\circ$. There is near-agreement of the six *P78-1* points with the Fe abundance of Phillips & Dennis (2011), determined from *RHESSI*. For the 19 *SMM* points, there is larger scatter, with the points spread between the curves for the Fe abundance of Phillips & Dennis (2011) and that of Feldman & Laming (2000). We note that the theoretical curves in Figure 2 for $h = 7000$ km would be about 20% lower than the appropriate solid curves, so if the mean flare height is of this order, the coronal Fe abundance is slightly less.

An estimate of the Fe abundance can be made from the *SMM* and *P78-1* ratios by comparing for each observation the

Table 2. Flares with Fe K α line emission

<i>SMM</i> BCS Flares						
Flare no.	Date	Time (UT) count rate ¹	Ch. 7 <i>w</i> count rate	Ch. 2 K α count rate	Fe K α /Fe xxv <i>w</i> ratio R_{obs}	Heliocentric distance θ (°)
1...	1980 Apr 7	05:40	604 (6)	40 (2)	0.087 (6)	16
2...	1980 Apr 10	09:18	452 (7)	20 (1)	0.058 (4)	46
3...	1980 May 9	07:13	1057 (10)	68 (2)	0.085 (4)	36
4...	1980 May 21	21:01	1689 (14)	77 (2)	0.060 (2)	17
5...	1980 Jun 25	15:54	512 (8)	27 (1)	0.069 (4)	42
6...	1980 Jul 1	16:31	190 (4)	6 (1)	0.038 (10)	40
7...	1980 Jul 5	22:49	857 (10)	66 (3)	0.101 (9)	37
8...	1980 Jul 12	11:17	257 (5)	14 (1)	0.069 (7)	58
9...	1980 Jul 14	08:28	494 (7)	33 (2)	0.088 (6)	45
10...	1980 Jul 21	03:00	491 (7)	23 (1)	0.062 (4)	63
11...	1980 Aug 23	21:28	53 (3)	3 (1)	0.065 (25)	49
12...	1980 Aug 31	12:51	118 (4)	9 (1)	0.100 (16)	29
13...	1980 Sep 24	07:35	172 (4)	9 (1)	0.065 (10)	27
14...	1980 Oct 14	06:19	1719 (14)	87 (3)	0.067 (3)	16
15...	1980 Nov 5	22:35	525 (4)	33 (1)	0.083 (4)	10
16...	1980 Nov 7	04:55	182 (2)	11 (1)	0.076 (8)	58
17...	1980 Nov 11	21:00	287 (3)	18 (1)	0.083 (6)	16
18...	1980 Nov 12	02:52	139 (2)	13 (1)	0.123 (14)	17
19...	1980 Nov 12	17:05	45 (1)	2 (1)	0.051 (11)	20
<i>P78-1</i> SOLFLEX Flares						
Flare no.	Date	Time (UT)	Fe K α /Fe xxv <i>w</i> ratio R_{obs}	Heliocentric distance θ (°)		
1...	1979 Mar 22	13:43	0.057	30		
2...	1979 Mar 25	18:05	0.043	79		
3...	1979 May 2	17:03	0.049	60		
4...	1979 Nov 8	23:35	0.065	49		
5...	1980 May 18	01:11	0.061	26		
6...	1981 Apr 18	18:06	0.066	26		

² Numbers in parentheses are uncertainties in the last significant figure.

factor f that the photospheric Fe abundance must be multiplied by to obtain the measured ratio. For the *SMM* points, f varies from 1.25 to 3.75, and for the *P78-1* points from 1.70 to 2.62. Histograms of the two distributions of f are given in Figure 5. Best-fit Gaussian curves to each distribution indicates that f for the *SMM* points is 1.6 ± 0.5 and for the *P78-1* points 2.0 ± 0.3 . There is thus some evidence for a small ($\sim 24\%$) systematic difference between the *SMM* and *P78-1* ratios.

A source of this systematic difference is very likely to be the effective areas of the *SMM* BCS channels 2 and 7. In the analysis of Phillips et al. (1995), a rough estimate of the relative effective area uncertainties was given as $\sim 30\%$. Some corroboration of this is provided here by simultaneous measurements of the Fe xxv *w* line in channels 4 and 7, the line being strong in both channels despite the factor-of-4 smaller sensitivity of channel 4. The channel 4 to channel 7 ratio is plotted against flare number in Figure 6 (upper panel). Evidently the ratio is at least 20% less than one as expected if the measured effective areas were precisely correct. The channel 3 and channel 2 measured fluxes of the K α lines are more difficult to compare because of the weakness of the lines in channel 3 (lower panel). The ratio is consistent with unity (mean value 1.12), but the statistical uncertainty is $\sim 35\%$. In summary, the ratio of relative sensitivities of BCS channels 2 and 7 probably accounts for the discrepancy between the *SMM* and *P78-1* points in Figure 4.

5 CONCLUSIONS

The possibility of obtaining the flare-to-photospheric Fe abundance ratio using the fluorescence-formed Fe K α and K β lines and the Fe xxv *w* line, expressed in our earlier work (Phillips et al. 1994, 1995), is carried further here in the case of *SMM* Bent Crystal Spectrometer and *P78-1* SOLFLEX spectra in the 6.39–6.70 keV (1.85–1.94 Å) range. The six *P78-1* measurements of the Fe K α -to-Fe xxv *w* line ratio indicate a flare-to-photospheric Fe ratio of 2.0 ± 0.3 , while the 19 *SMM* measurements indicate a flare-to-photospheric Fe abundance ratio of 1.6 ± 0.5 . The slight difference is likely to be due to $\gtrsim 20\%$ errors in the relative effective areas of BCS channels 2 and 7. The flare-to-photospheric Fe ratio from the *P78-1* measurements alone is consistent, to within uncertainties, with recent estimates of the flare Fe abundance from *RHESSI* spectra (Phillips & Dennis

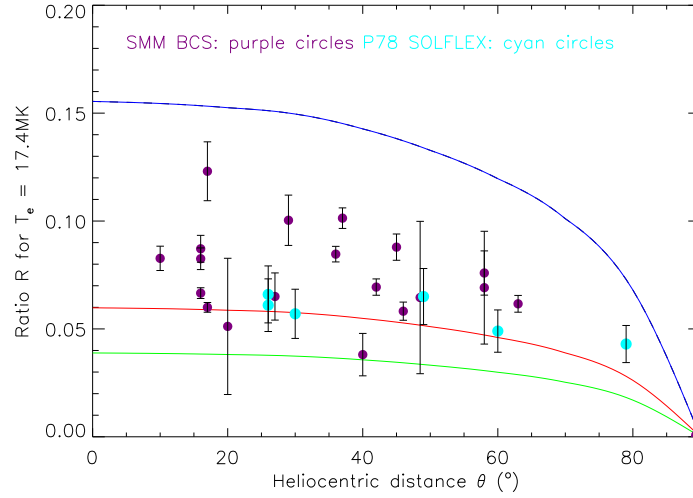


Figure 4. Observed ratios of Fe $K\alpha$ line flux (*SMM* BCS channel 2) to Fe XXV w line flux (channel 7) during flares listed in Table 2 plotted against flare heliocentric angle θ compared with theoretical curves calculated for zero height and for photospheric Fe abundance (blue), the flare abundance of Phillips & Dennis (2011) (red), and the coronal Fe abundance of Feldman & Laming (2000) (green). The *SMM* BCS points are in brown, the *P78-1* SOLFLEX points are in cyan (light blue). The corresponding $h = 7000$ km curves (not shown) are about 20% lower than the solid curves in this plot.

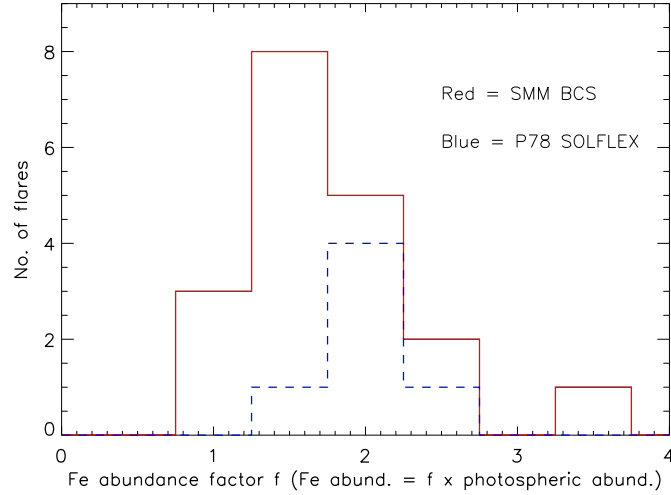


Figure 5. Histograms of Fe abundance factors f from *SMM* BCS and *P78-1* SOLFLEX spectra. The Fe abundance from each observation is f times the photospheric abundance of Asplund et al. (2009).

2011) which are a factor 2.6 ± 0.6 higher than the photospheric Fe abundance (Asplund et al. 2009; Caffau et al. 2011). This ratio is also consistent with *Yohkoh* Bragg Crystal Spectrometer measurements of the Fe $K\beta$ line (Phillips et al. 1995). These measurements of the Fe abundance enhancement may be relevant to the recent result of Wood & Linsky (2010) suggesting that FIP enhancements in active stars are greatest for Sun-like stars (spectral type G), decrease to zero for cool stars of type K0, while for later spectral types the coronal abundances of low-FIP elements are diminished relative to photospheric. The zero enhancement of Fe in the corona above a sunspot (Feldman et al. 1990) with effective temperature approximately equal to a K0 star and our own result for solar flares may fit such a picture.

ACKNOWLEDGMENTS

Much of the analysis of *SMM* BCS data has relied on the IDL routines written by D. M. Zarro, to whom thanks are due. I thank U. Feldman for use of the *P78-1* SOLFLEX data. CHIANTI is a collaborative project involving the US Naval Research Laboratory, the Universities of Florence (Italy) and Cambridge (UK), and George Mason University (USA).

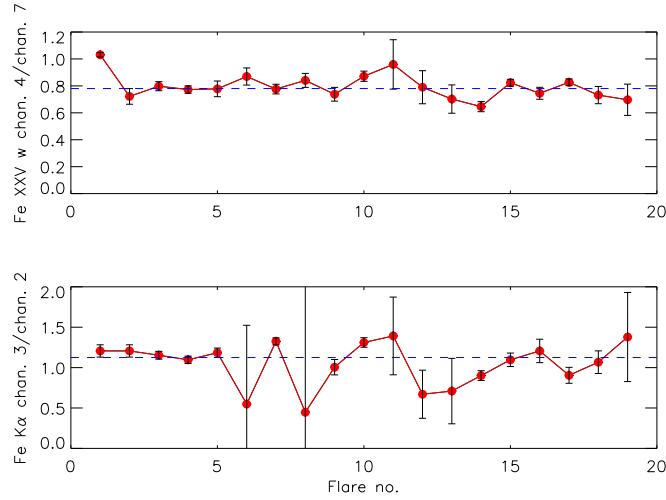


Figure 6. Upper panel: Ratio of fluxes in the Fe xxv line w estimated from *SMM* BCS channel 4 to channel 7 photon count rates with effective areas from Table 1. The mean ratio for these 19 observations is 0.78 ± 0.09 (blue horizontal line). Lower panel: Ratio of fluxes in the Fe K α lines estimated from *SMM* BCS channel 3 to channel 2 photon count rates and effective areas. The line is weak in particularly channel 3 and so the mean ratio, 1.12 ± 0.35 (blue horizontal line), is poorly determined. In each case, fluxes were determined using effective areas in Table 1.

REFERENCES

- Acton, L. W., et al. 1980, *Solar Phys.*, 65, 53
 Asplund, M., Grevesse, N., Sauval, A. J., & Scott, P. 2009, *ARAA*, 47, 481
 Bai, T. 1979, *Solar Phys.*, 62, 113
 Bambynek, W., Crasemann, B., Fink, R. W., Freund, H. U., Mark, M., Swift, C. D., Price, R. E., & Rao, P. V. 1972, *Rev. Mod. Phys.* 44, 716
 Bely-Dubau, F., Dubau, J., Faucher, P., & Gabriel, A. H. 1982, *MNRAS*, 198, 239
 Blackwell, D. E., Lynas-Gray, A. E., & Smith, G. 1995, *A & A*, 296, 217
 Bryans, P., Landi, E., & Savin, D. W. 2009, *ApJ*, 691, 1540
 Caffau, E., Ludwig, H.-G., Steffen, M., Freytag, B., & Bonifacio, P. 2011, *Solar Phys.*, 268, 255
 Dere, K. P., Landi, E., Mason, H. E., Monsignori Fossi, B. C., & Young, P. R. 1997, *A & AS*, 125, 149
 Dere, K. P., Landi, E., Young, P. R., Del Zanna, G., Landini, M., & Mason, H. E. 2009, *A & A*, 498, 915
 Doschek, G. A., Kreplin, R. W., & Feldman, U. 1979, *ApJL*, 233, L157
 Emslie, A. G., Phillips, K. J. H., & Dennis, B. R. 1986, *Solar Phys.*, 103, 89
 Feldman, U. 1992, *Phys. Scr.*, 46, 202
 Feldman, U., & Laming, J. M. 2000, *Phys. Scr.*, 61, 222
 Feldman, U., Widing, K. G., & Lund, P. A. 1990, *ApJL*, 364, L21
 Fink, R. W., Jopson, R. C., Mark, H., & Swift, C. D. 1966, *Rev. Mod. Phys.*, 38, 513
 Parmar, A. N., Wolfson, C. J., Culhane, J. L., Phillips, K. J. H., Acton, L. W., Dennis, B. R., & Rapley, C. G. 1984, *ApJ*, 279, 866
 Phillips, K. J. H., & Dennis, B. R. 2011, *ApJ* (submitted)
 Phillips, K. J. H., & Neupert, W. M. 1973, *Solar Phys.*, 32, 209
 Phillips, K. J. H., Pike, C. D., Lang, J., Watanabe, T., & Takahashi, M. 1994, *ApJ*, 435, 888
 Phillips, K. J. H., Pike, C. D., Lang, J., Zarro, D. M., Fludra, A., Watanabe, T., & Takahashi, M. 1995, *Adv. Space Res.*, 15 (7), 33
 Vernazza, J. E., Avrett, E. H., & Loeser, R. 1981, *ApJS*, 45, 635
 Widing, K. G., & Cheng, C.-C. 1974, *ApJL*, 194, L111
 Wood, B. E., & Linsky, J. L. 2010, *ApJ*, 717, 1279

This paper has been typeset from a \LaTeX file prepared by the author.